

# Development of Compact Plasma Sprayed Coatings for High Temperature Solar Tower Receivers

David Merino-Millan<sup>1</sup>[\[https://orcid.org/0000-0002-4364-2279\]](https://orcid.org/0000-0002-4364-2279), Claudio J. Múñez<sup>1</sup>[\[https://orcid.org/0000-0001-9872-1612\]](https://orcid.org/0000-0001-9872-1612),  
Miguel Ángel Garrido-Maneiro<sup>1</sup>[\[https://orcid.org/0000-0003-3518-7525\]](https://orcid.org/0000-0003-3518-7525),  
and Pedro Poza<sup>1</sup>[\[https://orcid.org/0000-0002-0496-4902\]](https://orcid.org/0000-0002-0496-4902)

<sup>1</sup> DIMME – Durability and Mechanical Integrity of Structural Materials, ESCET, Rey Juan Carlos University, Spain

**Abstract.** The current developments in concentrating solar power are focused in the third generation. Increase the working temperature of the plants is the main objective for this new generation. For this new condition, alternative materials for the receivers must be explored. In this work, a nickel alloy coating has been fabricated using a compact plasma spray system to be used on the receiver. This thermal spray system could be used for in-situ maintenance and overhaul as it is portable. Then the coatings have been exposed at high temperature of 800 °C, as expected in the third generation, during different exposure times. The evolution of the coating solar absorptivity and adherence have been studied over the selected exposure times. A maximum value of solar absorptivity 0.93 was reported for the longer exposure time studied. The adherence increment was remarkable reaching a value of about 57 MPa. These results show that these coatings could represent a durable alternative while the solar absorptivity maintains high values.

**Keywords:** Receiver, Absorptivity, Coatings, Thermal Spray, Concentrated Solar Power

## 1. Introduction

Today's energy needs are increasingly demanding renewable energy sources with the main goal of reducing carbon emissions. Thanks to this, the development of renewable energies is in full growth [1]. Among the renewable sources which currently concentrate more attention, the concentrated solar power (CSP) with central tower (CT) stands out. The main advantage of this technology is the energy storage capacity which make it available to be used according to the energy demand. However, this technology currently has the disadvantage of providing low energy efficiency. To improve this aspect, the current development line tends towards the so-called Generation 3 (Gen3) [2]. In this third generation, the CT plants are required to increase the working temperature, among other aspects, which generate problems for the materials currently used in the receivers.

Silicone-based paints are used as standard in most CSP plants [3]–[5]. The paint that stands out is Pyromark 2500. This paint gives the surface of the receiver high solar absorptivity (0.96) and is also easy to apply. However, at high temperatures >700 °C the paint degrades rapidly [6], making it unfeasible for Gen3 requirements [2], [7]. Rubino et al. [8] reviewed recently the use of thermal spray coatings as an alternative to silicon-base black paints.

Thermal spray coatings could be generated using a wide selection of materials depending on the desired properties. Frequently, the materials available have better resistance, stability and durability against the extreme conditions suffered in solar receivers. However, the application of thermal spraying coatings is not further employed for CT solar receivers.

The methodology proposed in this work is aimed to develop an alternative coating for solar receivers of central towers combining the use of Thermal Spray deposition with subsequent thermal treatments. The coatings will be fabricated using a Compact Plasma Spray system which would allow in-situ repairs. The effect of the isothermal exposition was evaluated at different remaining times inside oven. Solar absorptivity and adherence evolutions were studied.

## 2. Methodology

### 2.1 Materials

Amdry 625 powders (Oerlikon, USA) were used as raw materials to deposit the coatings. This powder has similar composition as commercial Inconel 625. The powder size distribution is -95+45  $\mu\text{m}$ , with round shape and was produced by gas atomization. The composition elements are shown in Table 1.

**Table 1.** Amdry 625 composition.

Element	Ni	Cr	Fe	Mo	Nb+Ta
Composition	Balance	21.5	2.5	9.0	3.7

### 2.2 Fabrication

The coatings were developed using a Compact Plasma Spray system (Sulzer, USA) with a maximum power output of 2500 W. This is a portable system but for this research it was mounted on a six-axis robotic arm KR900 (KUKA, Germany) in order to increase the reproducibility of the depositions. The deposits were performed onto AISI 316L stainless steel coupons with dimensions of 40 x 40 x 5 mm (width x height x thickness). The process parameters were previously optimized [9] and are presented in Table 2.

**Table 2.** Process parameters for deposit Inconel 625 with Compact Plasma System [9].

Parameter	Scanning Speed	Distance	Overlap	Plasma flow	Current	Powder Infeed
Values	0.018 m/s	128.5 mm	1 mm	0.88 NLPM	59 A	18.3 g/min

### 2.3 Heat treatment

After the deposition, the coupons were subjected to isothermal heat treatment at 800 °C. This temperature is desired for the third generation of concentrated solar power plants. The exposure times selected were 2, 4, 8, 12, 16 and 20 h. These times represents suitable times for industrial production. After this exposition times, the coupons remained inside the oven to allow slow cooldown until room temperature. In addition to heat treated coupons, extra as-sprayed coupons were deposited to be used as reference.

### 2.4 Solar absorptivity measurement

The solar absorptivity was measured using a reflectometer SOC-410 Solar (Surface Optics, USA) which conforms with ASTM E903 [10]. It measures the total reflectance between 400

and 1200 nm divided in four sub-bands. Then it reports the average solar absorptivity measured at 1.5 air mass.

## 2.5 Adherence test

The adherence between coating and substrate was measured using a testing machine PosiTest AT-A (Defelsko, USA). The measurements followed the recommendations of ASTM D4541 standard [11]. Two tests were executed for each coupon due to the limited space available. The dolly size employed was 10 mm in diameter and the adhesive used was an epoxy-based Araldite 170 GB. The stress rate applied was 2 MPa/s. The maximum resistance of the adhesive is  $57 \pm 9$  MPa.

## 2.6 Microstructural characterization

The metallographic characterization was performed on the cross-sectioned coupons which were hot mounted on thermoset resin. Each coupon was polished using a diamond slurry up to 1  $\mu\text{m}$  size.

The cross sectioned coupons were used to measure the coating thickness and characterize the internal microstructure. The thickness was measured using a Axioscope 5 (Zeiss, Germany) optical microscope and the software Zen 3.2 (Zeiss, Germany).

Also, the plane view and cross-section of the coupons were characterized using a scanning electron microscope (SEM) Hitachi S-3400 (Hitachi, Japan). Secondary electron (SE) and backscattered electron (BSE) images, with compositional contrast, were taken. Also, an energy dispersive X-ray microanalysis (EDX), attached to the SEM, was used.

Additionally, the surface composition was analyzed performing X-ray diffraction (XRD) tests onto the plain view surfaces of the coupons. A X'pert Pro diffractometer (PANalytical, Netherlands) was used with Cu-K $\alpha$  radiation and scanning angles between 10° to 115°, step size of 0.04 and 1 s per step.

## 3. Results and discussion

### 3.1 Microstructure

The microstructure of the coupons was evaluated on the cross section and the plain view of the coupons. The average thickness measured in the coupons was  $351 \pm 91$   $\mu\text{m}$ . In order to identify the phase formation onto the surface, Figure 1 represents the XRD patterns of different conditions studied. The main phases found were identified as  $\gamma$ -Ni (ICDD 01-077-9326), Cr<sub>2</sub>O<sub>3</sub> (ICDD 00-006-0504) and NiO (ICDD 00-004-0835). Cr<sub>2</sub>O<sub>3</sub> is primary formed, during the deposition process, surrounding the Inconel alloy areas. This formation can be seen in Figure 2 (a) where Inconel alloy is identified as (I) and Cr<sub>2</sub>O<sub>3</sub> is identified as (II). When the coupons are heat treated, alloy areas (I) evolve to rough areas marked as (III) in Figure 2 (b, c and d). The longer the exposure time, the bigger the roughness found.

On the as-sprayed coupons,  $\gamma$ -Ni and Cr<sub>2</sub>O<sub>3</sub> were identified.  $\gamma$ -Ni represents the matrix of the Inconel 625 alloy and Cr<sub>2</sub>O<sub>3</sub> is formed during plasma spraying. Figure 2 (a.1) shows the formation of these two phases marked as (I) for Inconel alloy and (II) for Cr<sub>2</sub>O<sub>3</sub>. It is usual that Cr<sub>2</sub>O<sub>3</sub> is formed when Inconel 625 is thermally sprayed because it is easily formed at temperatures above 550 °C [12], [13]. However, when the coating is exposed at temperatures above 750 °C a new oxide phase is formed, NiO [12], [13]. Heat-treated coupons have shown the formation of NiO on the XRD in Figure 1. These NiO areas are formed from the exposed Inconel alloy areas marked as (I) in Figure 2 when it is heat-treated. The new NiO areas are marked as (III) in Figure 2 for the heat-treated coupons.

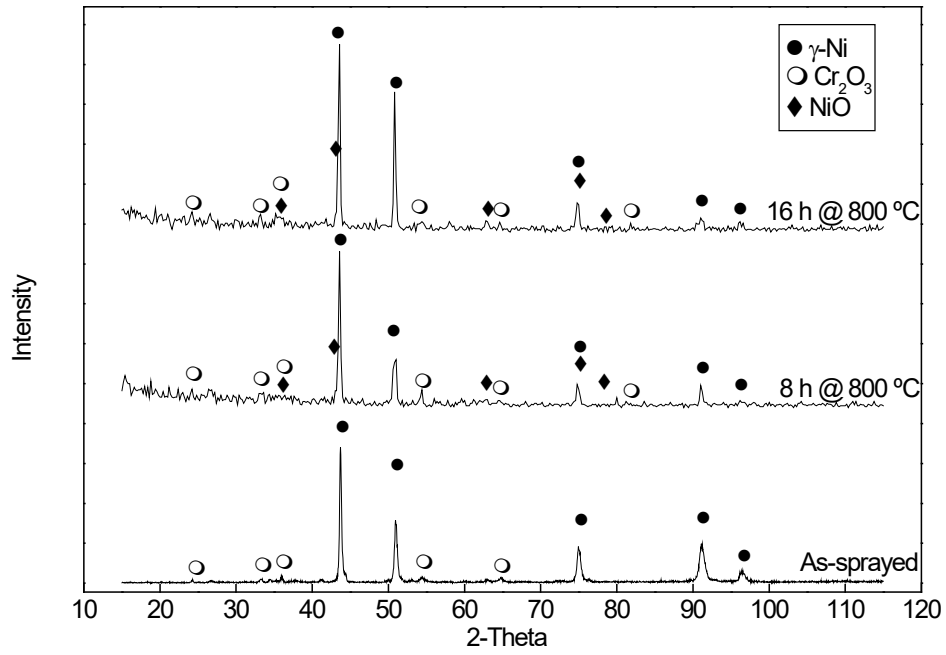


**Figure 1.** Plain view XRD pattern for as-sprayed, 8 h and 16 h heat treated coupons.

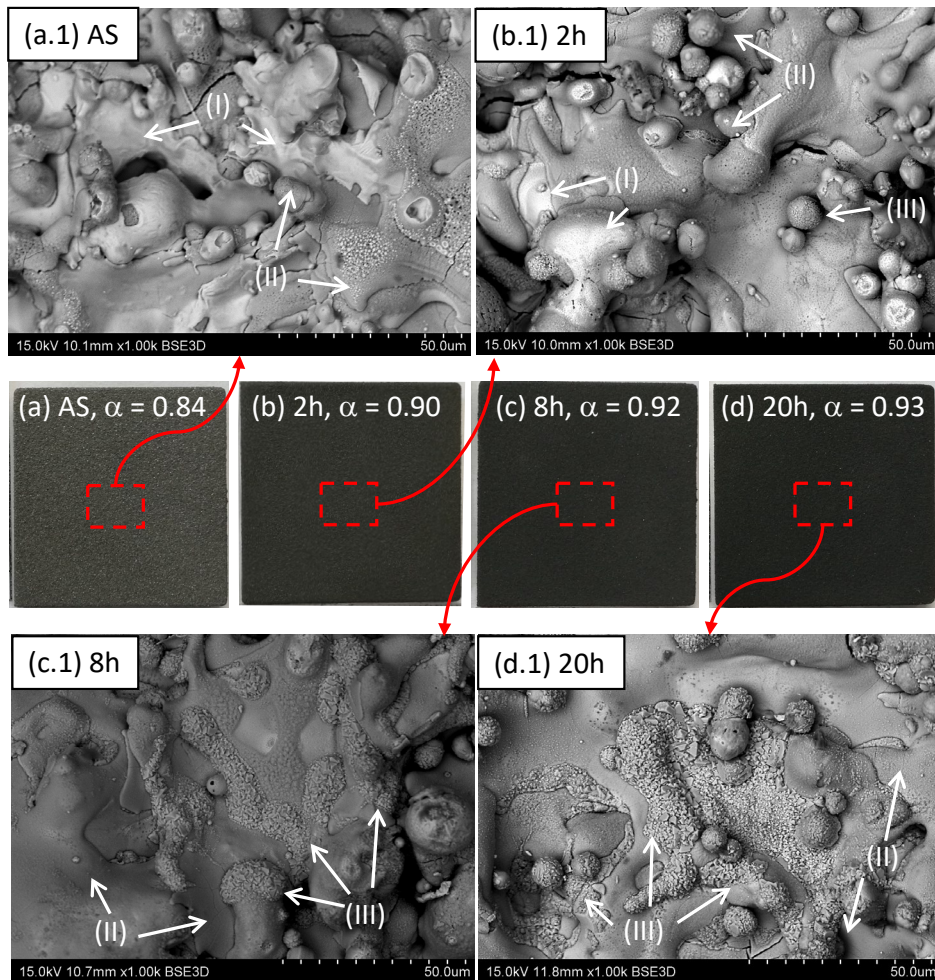


**Figure 2.** Surface appearance of as-sprayed (a) and heat treated for 2 h (b), 8 h (c) and 20 h (d) coupons and its BSE images. The marks represent areas of Inconel alloy (I), Cr<sub>2</sub>O<sub>3</sub> (II) and NiO (III).

These crystal shaped NiO areas grow slowly over exposure time by extension and crystal size. Figure 3 represents the evolution of the NiO crystals size over consecutive exposure times. These crystals contribute on the roughness of the coupon which could contribute on the light retention, increasing the absorptivity.

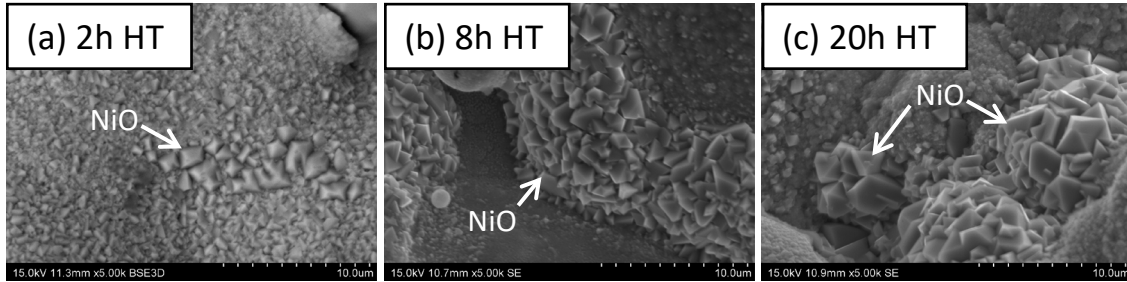


**Figure 3.** NiO formation on the plain view heat-treated coupons of 2 (a), 8 (b) and 20 h (c).

### 3.2 Adherence

The adherence results are shown in Figure 4. The values of the as sprayed coupons reached 25 MPa. The heat-treated coupons report an increment, just after 2 h of high temperature exposure, reaching about 51 MPa. For exposure times longer than 2 h, the values of adherence show the failure of the adhesive about 57 MPa. It does not represent the actual adhesion of the coating but it means that the adherence would be above this value.

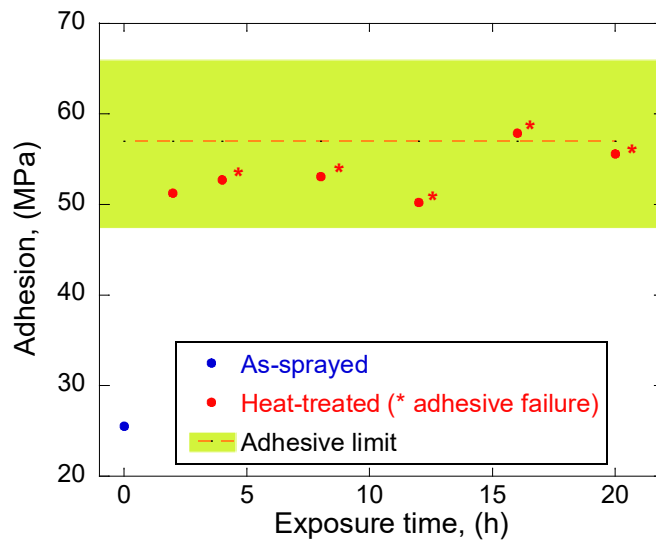


**Figure 4.** Adhesion measured for as-sprayed and HT coatings.

These adherence increments for the heat-treated coatings are caused by diffusion at the coating-substrate interface. The diffusion between the main elements of the Inconel alloy (Ni, Cr and Fe) and the elements in the substrate (Fe, Cr and Ni) happens easily when they are in contact [14]. The elements which diffused were nickel and iron. The chromium composition is similar in both coating and substrate, so the diffusion mechanisms are limited. Figure 5 shows a representative EDX compositional line scan in the interface area for a 20 h HT coupon. The graph represents the relative composition of elements. The diffusion area was highlighted in

blue where the diffusion mechanisms between Ni and Fe come about. Fe diffuses from substrate to the coating and Ni, from coating to the substrate. This phenomenon is more remarkable on longer exposition times.

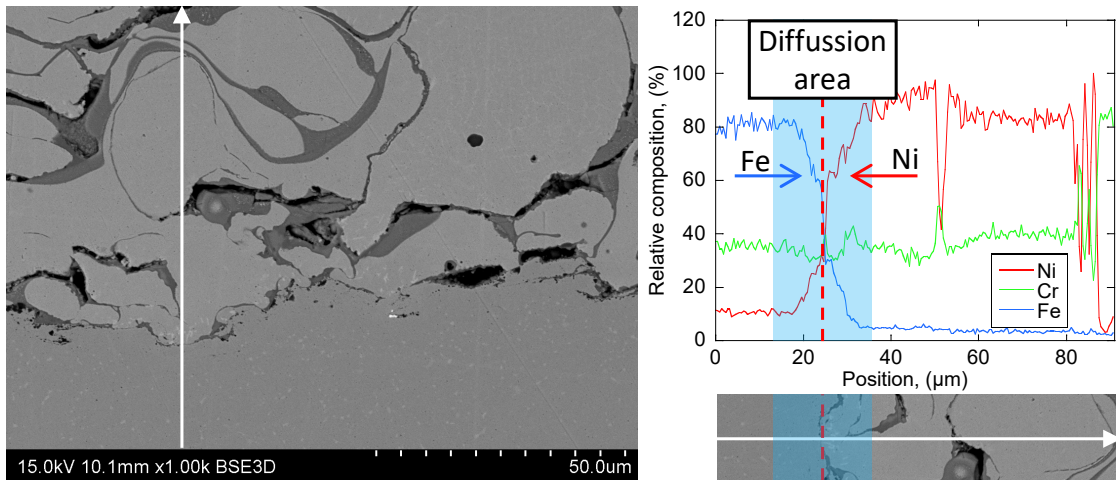


**Figure 5.** EDX compositional line scan of the interface area coating-substrate for a 20 h heat-treated coupon.

### 3.3 Solar absorptivity

Figure 6 represents the solar absorptivity versus exposure times. The as sprayed coupons reported a value of 0.83 while the 20 h heat-treated coupons reached the value of 0.93. The solar absorptivity increases over exposure time following a logarithmic growth.

The oxides formed during the thermal spray process and subsequent heat treatments contributes on darkening the surface.  $\text{Cr}_2\text{O}_3$  and  $\text{NiO}$ , formed on the surface, have solar absorptivities of about 0.92 and 0.97, respectively [15]. The relative surface coverage of the coating contributes on increasing the solar absorptivity. This relative contribution has been studied by Merino et al. [9] using the rules of mixtures. The extensive the  $\text{NiO}$  formation, the higher coating solar absorptivity.

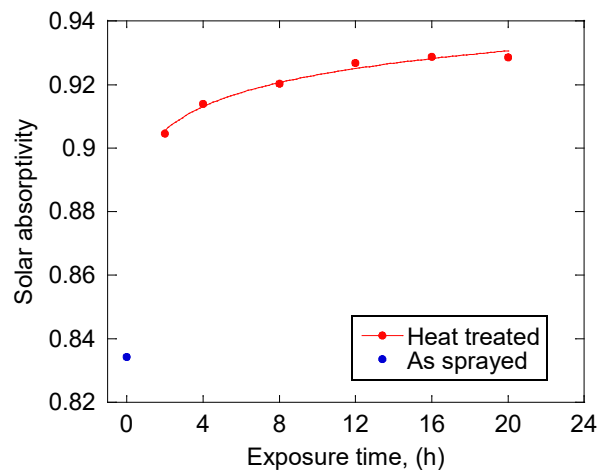


**Figure 6.** Solar absorptivity measured for as-sprayed and heat-treated coatings.

## 4. Conclusions

- A coating of Inconel 625 has been successfully fabricated using a Compact Plasma Spray system and the functional and mechanical properties has been enhanced by isothermal heat treatment.
- Solar absorptivity has been improved from 0.83 to 0.93 by just 20 hours of heat treatment, due to the formation of nickel and chromium oxides onto the exposed surface of the coating.
- The adherence of the coating has been increased during the isothermal exposition up to values over 57 MPa.
- The heat treatment performance has been evaluated. 8 h exposure time is proposed as the most recommendable. It is the shortest time at which the adherence is in the maximum and the solar absorptivity is almost on the asymptotic value.
- This coating could represent a feasible alternative to silicon-based paints due to its estimated high durability and despite the absorptivity.
- The formation of these high absorbent oxides could be formed *in-situ* during plant operation.

## Data availability statement

No data available.

## Author contributions

David Merino-Millan: Writing – original draft, Writing – review & editing, Methodology, Investigation, Formal analysis, Data curation, Conceptualization. Claudio J. Múñez: Writing – review & editing, Resources, Project administration, Methodology, Funding acquisition, Conceptualization. Miguel Ángel Garrido-Maneiro: Writing – review & editing, Methodology, Conceptualization, Funding acquisition. Pedro Poza: Writing – review & editing, Supervision, Methodology, Conceptualization, Funding acquisition.

## Competing interests

The authors declare no competing interests.

## Funding

The authors wish to thank to “Comunidad de Madrid” and European Structural Funds for their financial support of ACES2030-CM project (S2018/EMT-4319). The authors also acknowledge financial support received from the Spanish government AEI under Grant No. PID2020-115508RB-C22 (A3M).

## References

1. IRENA, *Renewable capacity statistics 2021 International Renewable Energy Agency (IRENA)*. Abu Dhabi, 2021.
2. Y. L. He *et al.*, “Perspective of concentrating solar power,” *Energy*, vol. 198, p. 117373, 2020, doi: 10.1016/j.energy.2020.117373.
3. A. Boubault, C. K. Ho, A. Hall, T. N. Lambert, and A. Ambrosini, “Durability of solar absorber coatings and their cost-effectiveness,” *Sol. Energy Mater. Sol. Cells*, vol. 166,

- no. March 2017, pp. 176–184, 2017, doi: 10.1016/j.solmat.2017.03.010.
4. A. Ambrosini, A. Boubault, C. K. Ho, L. Banh, and J. R. Lewis, "Influence of application parameters on stability of Pyromark®2500 receiver coatings," 2019, p. 30002, doi: 10.1063/1.5117514.
  5. C. K. Ho, A. R. Mahoney, A. Ambrosini, M. Bencomo, A. Hall, and T. N. Lambert, "Characterization of Pyromark 2500 Paint for High-Temperature Solar Receivers," *J. Sol. Energy Eng.*, vol. 136, no. 1, pp. 2014–2017, 2014, doi: 10.1115/1.4024031.
  6. N. Martínez, A. Rico, C. J. Múnez, C. Prieto, and P. Poza, "Improving durability of silicone-based paint coatings used in solar power plants by controlling consolidation procedures," *Sol. Energy*, vol. 199, no. September 2019, pp. 585–595, 2020, doi: 10.1016/j.solener.2020.02.049.
  7. C. K. Ho and B. D. Iverson, "Review of high-temperature central receiver designs for concentrating solar power," *Renew. Sustain. Energy Rev.*, vol. 29, pp. 835–846, 2014, doi: 10.1016/j.rser.2013.08.099.
  8. F. Rubino, P. Poza, G. Pasquino, and P. Carlone, "Thermal spray processes in concentrating solar power technology," *Metals (Basel)*, vol. 11, no. 9, pp. 1–30, 2021, doi: 10.3390/met11091377.
  9. D. Merino-Millan, C. J. Múnez, M. Á. Garrido-Maneiro, and P. Poza, "Alternative low-power plasma-sprayed inconel 625 coatings for thermal solar receivers : Effects of high temperature exposure on adhesion and solar absorptivity," *Sol. Energy Mater. Sol. Cells*, vol. 245, no. June, 2022, doi: 10.1016/j.solmat.2022.111839.
  10. ASTM International, "ASTM E903-20, Standard Test Method for Solar Absorptance , Reflectance , and Transmittance of Materials Using Integrating Spheres," vol. 03. West Conshohocken, PA, pp. 1–9, 2020, doi: 10.1520/E0903-20.
  11. ASTM International, "ASTM D4541-17, Standard Test Method for Pull-Off Strength of Coatings Using Portable Adhesion Testers," *ASTM International*. West Conshohocken, PA, pp. 1–16, 2017, doi: 10.1520/D4541-17.
  12. M. Balat-Pichelin, J. L. Sans, E. Bêche, L. Charpentier, A. Ferrière, and S. Chomette, "Emissivity at high temperature of Ni-based superalloys for the design of solar receivers for future tower power plants," *Sol. Energy Mater. Sol. Cells*, vol. 227, no. July 2020, 2021, doi: 10.1016/j.solmat.2021.111066.
  13. A. M. de Sousa Malafaia, R. B. de Oliveira, L. Latu-Romain, Y. Wouters, and R. Baldan, "Isothermal oxidation of Inconel 625 superalloy at 800 and 1000 °C: Microstructure and oxide layer characterization," *Mater. Charact.*, vol. 161, no. October 2019, p. 110160, 2020, doi: 10.1016/j.matchar.2020.110160.
  14. A. Durand, L. Peng, G. Laplanche, J. R. Morris, E. P. George, and G. Eggeler, "Interdiffusion in Cr–Fe–Co–Ni medium-entropy alloys," *Intermetallics*, vol. 122, p. 106789, 2020, doi: 10.1016/j.intermet.2020.106789.
  15. C. Atkinson, C. L. Sansom, H. J. Almond, and C. P. Shaw, "Coatings for concentrating solar systems - A review," *Renew. Sustain. Energy Rev.*, vol. 45, pp. 113–122, 2015, doi: 10.1016/j.rser.2015.01.015.